Tracking by Shape with Deforming Prediction for Non-rigid Objects

Kenji Nishida[1], Takumi Kobayashi[1] and Jun Fujiki[2]
[1]*National Institute of Advanced Industrial Science and Technology (AIST), Tsukuba, Japan*
[2]*Department of Applied Mathematics, Fukuoka University, Fukuoka, Japan*

Keywords: Tracking, Deforming Objects, Shape Prediction, Motion Feature.

Abstract: A novel algorithm for tracking by shape with deforming prediction is proposed. The algorithm is based on the similarity of the predicted and actual object shape. Second order approximation for feature point movement by Taylor expansion is adopted for shape prediction, and the similarity is measured by using chamfer matching of the predicted and the actual shape. Chamfer matching is also used to detect the feature point movements to predict the object deformation. The proposed algorithm is applied to the tracking of a skier and showed a good tracking and shape prediction performance.

1 INTRODUCTION

Visual object tracking is used in a wide range of computer vision applications, such as surveillance systems, intelligent transport systems, and human action analysis. The primary function of an object tracking algorithm is to find the regions in an image that contain movements. Therefore, in the first approach, proposed by Koller, a background subtraction algorithm was employed (Koller et al. 1994). However, in this approach, the performance of the background estimation was degraded when the movement of the objects was small, and it also required an appropriate illumination condition.

The second approach comprises a group of feature-based tracking algorithms (Beymer et al. 1997; Coifman et al. 1998; Kim and Malik, 2003). Salient features such as corner features are individually extracted and tracked are grouped as belonging to the corresponding object. It can be robust to illumination change. However, the precision of the object location and dimension is affected by the difficulties that arise in feature grouping. Another feature-based approach is called the mean-shift algorithm (Comaniciu and Meer, 2002; Comaniciu et al. 2000), in which the local features (such as color histograms) of pixels belonging to the object are followed. The mean-shift approach allows robust and high-speed object tracking, if a local feature that successfully discriminates the object from the background exists. However, it is difficult to discriminate objects that are close to each other and are similar in color, or to adopt this method for gray-scale images.

The third approach can be classified as a detect-and-track approach. Avidan redefined the tracking problem as that of classifying (or discriminating between) the objects and the background (Avidan, 2002). In this approach, features are extracted from both the objects and the background; then, a classifier is trained to classify (discriminate between) the object and the background. Grabner trained a classifier to discriminate an image patch with an object in the correct position and image patches with objects in the incorrect position (Grabner, 2006), and thereby, the position of the object could be estimated more precisely. While this approach allows stable and robust object tracking, a large number of computations are necessary. The approach of Collins and Mahadevan is classified as an approach of this type, but they selected discriminative features instead of training classifiers (Collins et al. 2005; Mahadevan and Vasconcelos, 2009). Grabner introduced on-line boosting to update feature weights to attain compatibility between the adaptation and stability for the appearance change (illumination change, deformation, etc.) of tracking classifiers (Grabner et al. 2008). Woodley employed discriminative feature selection using a local generative model to cope with appearance change while maintaining the proximity to a static appearance model (Woodley et al. 2007). The tracking algorithms are also applied to the non-rigid (deforming) objects. Godec proposed *Hough-based tracking* algorithm for non-rigid objects, which employed Hough voting to determine the object's position in the next

Nishida K., Kobayashi T. and Fujiki J..
Tracking by Shape with Deforming Prediction for Non-rigid Objects.
DOI: 10.5220/0004813305800587
In *Proceedings of the 3rd International Conference on Pattern Recognition Applications and Methods* (ICPRAM-2014), pages 580-587
ISBN: 978-989-758-018-5

frame (Godec et al. 2013).

In detect-and-track approaches, the estimated object position in the next video frame is determined based on the similarity of the features to the object in the current video frame, and a change in appearance, especially deformation, may affect the similarity between the object in the current and the next frame, and thereby, the accuracy of the tracking. Therefore, the tracking accuracy can be improved by predicting the deformation of the object to improve the similarity of the object in the next video frame to that in the current video frame. Sundaramoorthi proposed a new geometric metric for the space of closed curves, and applied it to the tracking of deforming objects (Sundarmoorthi et al. 2010). In this algorithm, the deforming shapes of the objects are predicted from the movement of the feature points using first order approximation. Therefore, it should be classified as a *predict-and-track* approach.

In this paper, we propose a novel predict-and-track algorithm based on shape prediction using second order approximation. In our algorithm, the objects are tracked on the basis of the object shape, which is represented by the outline edge, and the chamfer distance is employed as a similarity measure of the object shape in the current and the next video frame. Our algorithm is applied to the tracking of a skier, which involves a significant deformation and some partial occlusions.

The rest of this paper is organized as follows. First, in section 2 we describe our shape prediction algorithm and the tracking procedure using chamfer distance as a similarity measure. Next, the experimental results are shown in section 3. Then, the discussion and future work are presented in section 4. Finally, we present our conclusions in section 5.

2 SHAPE PREDICTION AND TRACKING ALGORITHM

An algorithm for tracking by shape prediction is described in this section. The proposed algorithm consists of two components, shape prediction and tracking by shape similarity.

2.1 Notations

Here, we summarize the notation used in this paper.

- X denotes the center position of the object,
- $O(X)$ denotes the object image centered at position X,
- $E(X)$ denotes the edge image for the object at position X,
- $\hat{O}$ and $\hat{E}$ denote the predicted image and edge image for the object, respectively,
- x denotes the positions of the feature points for object X,
- x' denotes the differential of x such as $x' = \frac{dx}{dt}$,
- x'' denotes $\frac{d^2x}{dt^2}$,
- $\tilde{x}$ denotes the subset of feature points of the object that constitute the outline edge, $\tilde{x} \in E(X)$,
- $\hat{x}$ denotes the predicted position for $\tilde{x}$,
- $l(x)$ denotes the edgelet for position x.

2.2 Shape Prediction

We adopted a shape prediction algorithm based on the second order approximation of the feature points' movement as our tracking algorithm (Authors, submitted to VISAPP 2014).

When x_t is determined to be the 2-D position of the feature points that constitute the object image O at t, the position of the pixels at $t+1$ is estimated by Taylor expansion as

$$x_{t+1} = x_t + x'_t + \frac{1}{2}x''_t. \quad (1)$$

x' is usually called an optical flow, and it is practically computed as the difference in the pixel position:

$$x'_t = x_t - x_{t-1}. \quad (2)$$

Similarly, x'' denotes the second order differential of x, which is calculated as

$$\begin{aligned} x''_t &= x'_t - x'_{t-1} \\ &= x_t - x_{t-1} - (x_{t-1} - x_{t-2}) \\ &= x_t - 2x_{t-1} + x_{t-2}. \end{aligned} \quad (3)$$

Therefore, the appearance of the object at $t+1$ can be predicted based on the optical flows computed from three consecutive video frames. Suppose that the shape of the object is determined by the outline edge image E, which is predicted from the feature point movements in previous video frames. The algorithm for detecting the feature point movements is described in section 2.3.1.

2.3 Tracking by Predicted Shape

The movement of the feature points comprises both the object translation (the movement of the center of the object) and the movement of the pixels relative to the center of the object, for example,

$$x'_t = X'_t + r'_t, \quad (4)$$

where X denotes the position of the object's center, and r denotes the position of the pixels relative to the object's center. The purpose of our tracking algorithm is to determine the next object position X_{t+1} using the similarity between the predicted and actual object shape. The relative movement r' affects the object deformation, which contributes significantly in the prediction of the object shape. Figure 1 shows the movement of the feature point x', the movement of the object's center, X', and the relative movement r'.

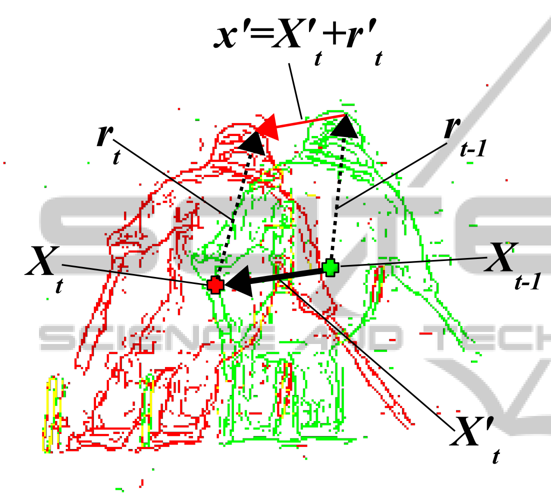

Figure 1: Edge image and object movement.
Green: Edge image for $t-1$, Red: Edge image for t

The similarity between the predicted edge image $\hat{E}_{t+1}$ and actual edge image E_{t+1} is measured by using the Chamfer System (Gavrila, 2000). The Chamfer System measures the similarity of two edge images using distance transform methodology (DT) (Huttenlocher et al. 1993).

Let us consider the problem of measuring the similarity between template edge image E_t (fig. 2(b)) and a succeeding edge image E_{t+1} (fig. 2(c)). We apply the distance transform to obtain a DT image D_{t+1} (fig. 2(d)), where each pixel value d_{t+1} denotes the distance to the nearest feature pixel of E_{t+1}. The chamfer distance, $D_{chamfer}$, is defined as

$$D_{chamfer}(E_t, E_{t+1}) = \frac{1}{|E_t|} \sum_{e \in E_t} d_{t+1}(e) \quad (5)$$

where $|E_t|$ denotes the number of feature points in E_t, e denotes a feature point of E_t, and $d_{t+1}(e)$ denotes the chamfer distance between feature point e and E_{t+1}.

The translation of the object can be detected by finding the position of the predicted edge image $\hat{E}_{t+1}$ that minimizes the chamfer distance between it and the actual edge image E_{t+1}.

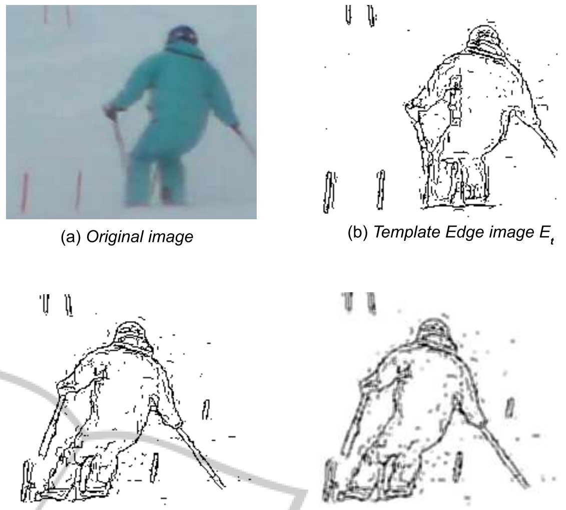

(a) Original image (b) Template Edge image E_t

(c) Next Edge image E_{t+1} (d) DT image D_{t+1}

Figure 2: Chamfer system.

$$X_{t+1} = \arg\min_{X_{t+1}} D_{chamfer}(\hat{E}_{t+1}(X_{t+1}), E_{t+1}). \quad (6)$$

Figure 3 shows the tracking procedure, where the blue edge represents the predicted edge image $\hat{E}$, the red edge represents the actual edge image E, and the green edge represents the translated predicted edge image $\hat{E}(X)$ according to equation (6).

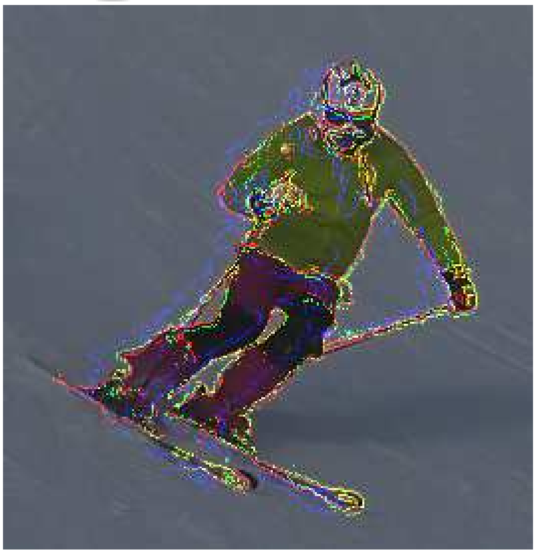

Figure 3: Tracking procedure.
Blue: predicted edge image; Green: translated predicted edge image; Red: reconstructed edge image.

2.3.1 Detection of Relative Movement

After the object translation X'_{t+1} is determined, the relative movements of the feature points r'_{t+1} are detected to determine the feature point movement x'_{t+1}. The relative movement r'_{t+1} is detected using the actual edge image at $t+1$ by tracking small parts of the edge (edgelets). We also employed the Chamfer System (Gavrila, 2000) to detect the relative movement of the edgelets.

When a template edgelet image $l(\tilde{x}_t)$ is extracted from E_t, the candidate edgelet $l(\tilde{x}_t + X'_{t+1} + \hat{r}'_{t+1})$ is extracted from next edge image E_{t+1} using X' as an offset. The deformation of the object can be detected by finding the edgelet pair such that the chamfer distance between the edgelet image in $l(\tilde{x}_t)$ and the corresponding edgelet image in $l(\tilde{x}_t + X'_{t+1} + \hat{r}'_{t+1})$ (fig. 4):

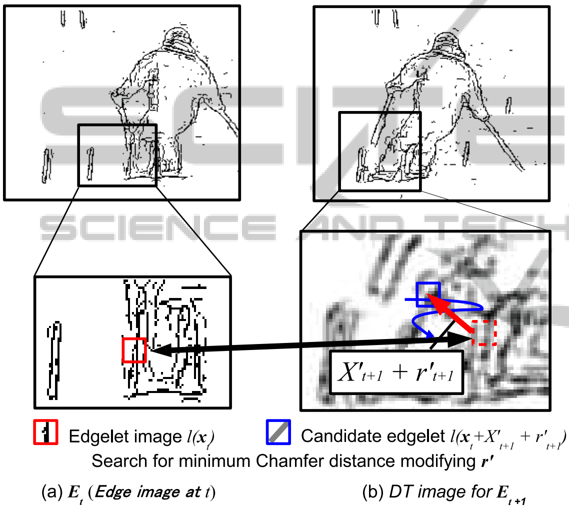

Figure 4: Edgelet tracker.

$$\hat{r}'_{t+1} = \arg\min_{\hat{r}'_{t+1}} D_{chamfer}(l(\tilde{x}_t), l(\tilde{x}_t + X'_{t+1} + \hat{r}'_{t+1})), \tag{7}$$

Since the detected relative movements $\hat{r}'_{t+1}$ may contain some noise, smoothing is applied by taking an average of the relative movements in the neighboring region.

$$r'_{t+1} = \frac{1}{N} \sum_{\hat{r}'_{t+1} \in \delta_{t+1}} \hat{r}'_{t+1}, \tag{8}$$

where N stands for the number of detected relative movements $\hat{r}'_{t+1}$ in the neighborhood δ of $\tilde{x}_t$.

Finally, the feature point movement x'_{t+1} is determined by summing the object translation X'_{t+1} and the relative movement r'_{t+1},

$$x'_{t+1} = X'_{t+1} + r'_{t+1}. \tag{9}$$

3 EXPERIMENTAL RESULTS

The proposed algorithm was applied to two video sequences of skiing, one of which was a sequence captured by a hand-held camera, while the other was a sequence captured by a fixed camera. The effect of the ego-motion of the camera was examined in the sequence of the hand-held camera, and the tracking performance for the skier's movement was examined in the sequence of the fixed camera.

3.1 Video Sequence of Hand-held Camera

We first examined the video sequence captured by the hand-held camera. In this sequence, the skier was manually tracked so as to be shown near the center of the image frame, and thus, the object tends to have a small translation in the image frame. However, the object sometimes has a large translation caused by the mis-tracking of the camera. Figure 5 shows the tracking result. The blue edge represents the predicted object shape, the green edge represents the translated predicted shape to determine the object position using equation (6), and the red edge represents the reconstructed object shape, which is calculated by equation (1) using the result of the final estimation obtained using equation (9).

The results show that the proposed algorithm successfully tracked the object with good prediction of the shape. In the prediction phase for frame number 392, there was a significant error in the position estimation, which may have been caused by the large ego-motion that occurred between frames 391 and 392. However, the position of the object was corrected by finding the appropriate position using chamfer matching between the predicted and the actual edge image. The detected movements of the feature points can be verified by the reconstructed edge image.

3.2 Video Sequence of Fixed Camera

Figure 6 shows the results for the video sequence captured by the fixed camera. Since the skier was not tracked by the camera, the translation of the skier had to be tracked. Although the results show that the object was tracked successfully, there was some errors in the shape prediction and reconstruction, such as that of the legs in frames 52 and 54. It is considered that difference in the movement of the ski pole and the skier's legs, which were very close together in frames 52 and 54, caused this error.

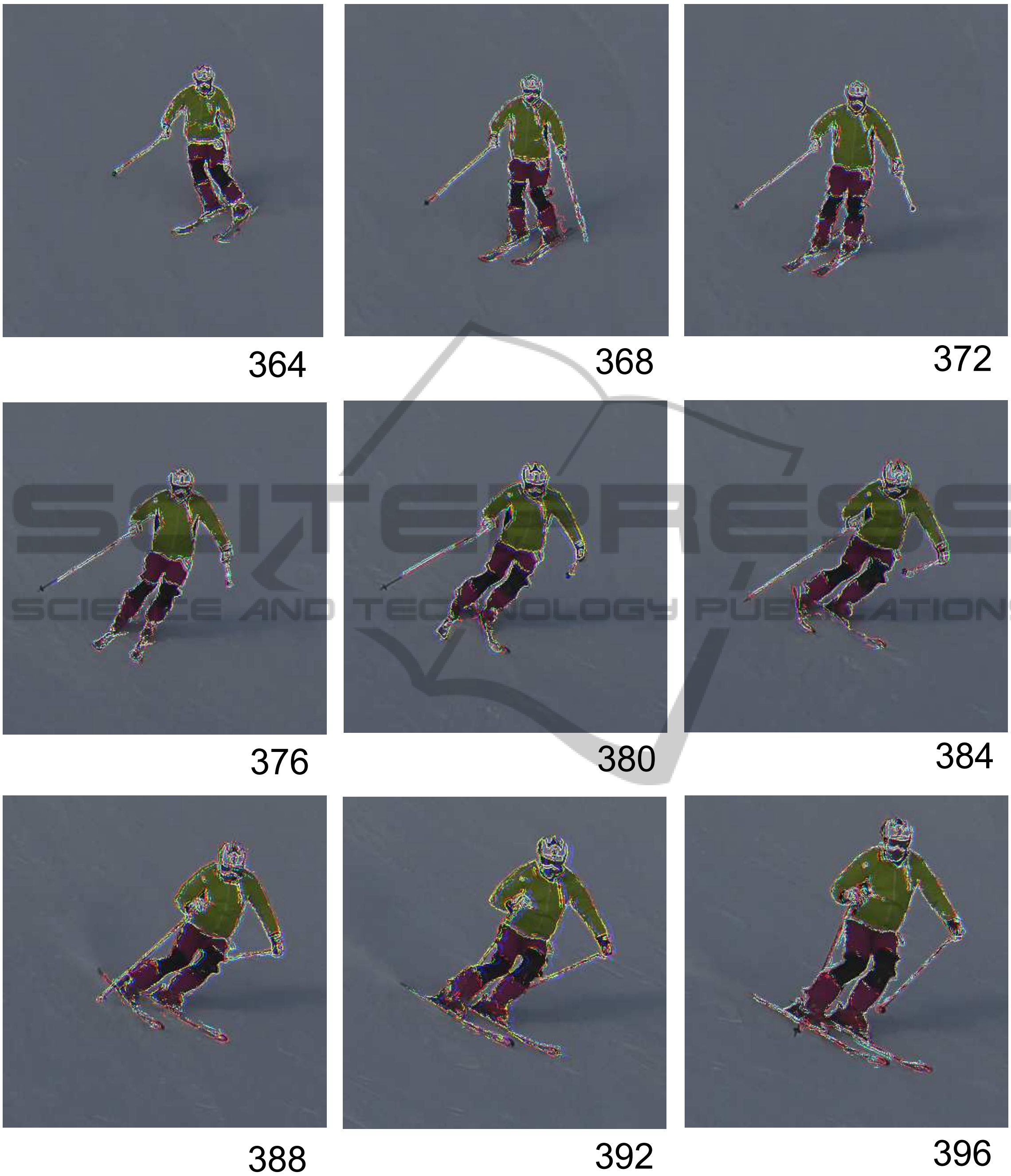

Figure 5: Tracking result for Hand-held camera.
Blue: predicted edge image; Green: translated predicted edge image; Red: reconstructed edge image.

4 DISCUSSION AND FUTURE WORK

Although in some previous studies on shape prediction, such as those of (Sim and Sundaraj, 2010) and (Sundarmoorthi et al. 2010), only a first order differential (optical flow) was adopted, we adopted up to second order differentials for shape prediction.

The effect of second order differentials is indicated in fig. 7, where the blue edge represents the ground truth, the green edge represents the prediction when only the first order differential is adopted, and the red edge represents the prediction with up to sec-

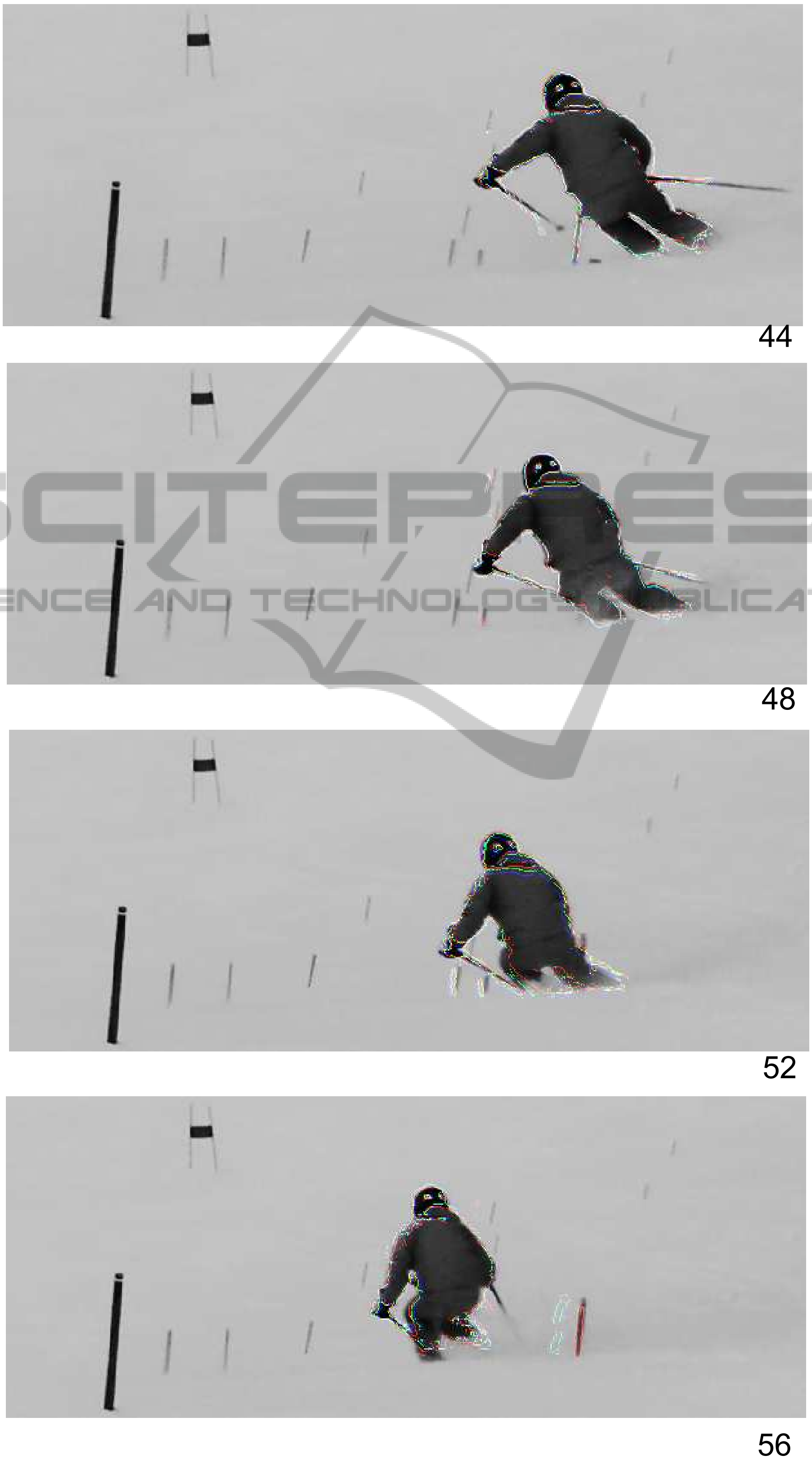

Figure 6: Tracking result for fixed camera.
Blue: predicted edge image; Green: translated predicted edge image; Red: reconstructed edge image.

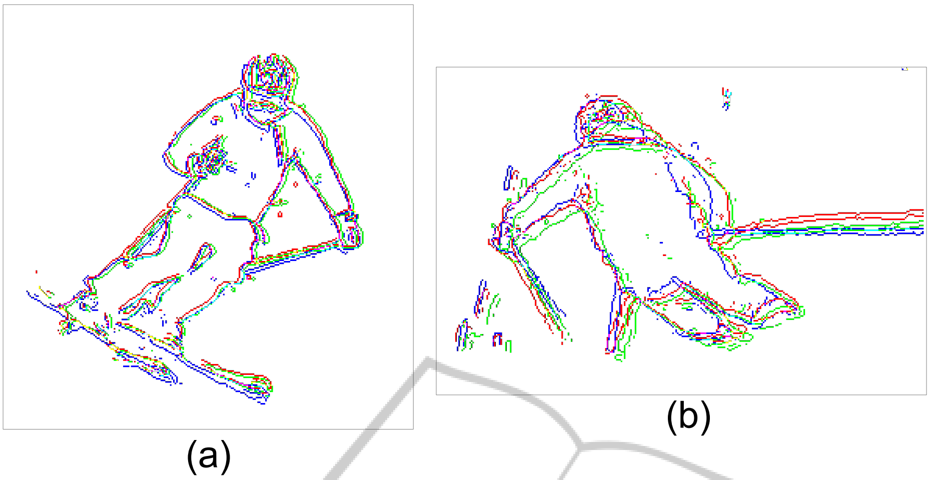

Blue: Ground truth, Green: Prediction w/o 2nd Order Approx., Red: Prediction with 2nd order Approx.

Figure 7: Effect of 2nd order approximation for shape prediction.

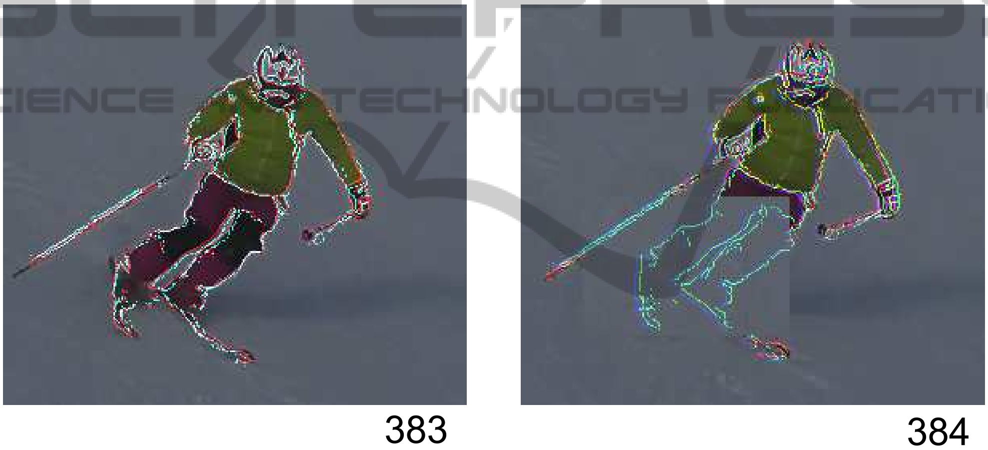

Figure 8: Occlusion recovery.

ond order differentials. Both the results in fig. 7 indicate that the shape prediction accuracy was improved by adopting the second order differential.

Occlusion recovery is one of the important issues related to tracking algorithms. Since our algorithm predicts the object shape from the preceding video frames, it is possible to predict the shape of an occluded object. Figure 8 shows that the proposed algorithm predicts the shape of the object that is artificially occluded in video frame 384.

5 CONCLUSIONS

In this paper, we proposed a tracking algorithm using shape matching between the predicted and the actual object in the next video frame. In the proposed algorithm, second order approximation for shape prediction was adopted and the algorithm attained a good tracking performance. Because of the accurate shape prediction, the proposed algorithm showed that it is possible to recover the shape of an object in occluded regions.

REFERENCES

Authors, submitted to VISAPP 2014.

S.Avidan, “Ensemble Tracking”, *IEEE PAMI*, Vol.29, No.2, pp.261,271, 2007.

D.Beymer, et al., “A Real-Time Computer Vision System for Measuring Traffic Parameters”, in *Proc. IEEE CVPR*, pp.495-501, 1997.

T. Brox, C. Bregler, and J. Malik, “Large Displacement Optical Flow”, in *Proc. CVPR 2009*, pp. 41-48, 2009.

B.Coifman, et al., “A Real-time Computer Vision System for Vehicle Tracking and Traffic surveillance", *Transportation Research Part C*, No.6, pp.271-288, 1998.

R.T.Collins, et al., "Online Selection of Discriminative Tracking Features", in *IEEE PAMI*, Vol.27, No.10, pp.1631-1643, 2005.

D. Comaniciu, V. Ramesh, and P. Meer,. "Real-Time Tracking of Non-Rigid Objects using Mean Shift", in *Proc. CVPR 2000*, pp. 142-149, 2000.

D.Comeniciu, P.Meer, "MeanShift: A Robust Approach Toward Feature Space Analysis", *IEEE PAMI*, Vol.24, No.5, pp.603-619, May, 2002.

D.M. Gavrila, "Pedestrian Detection from a Moving Vehicle", in *Proc. ECCV 2009*, pp. 37-49, 2009.

M. Godec, P.M Roth, and H.Bischof, "Hough-based Tracking on Non-rigid Objects", to appear in *J. of Computer Vision and Image Understanding*, available online, Elsevier, 2013.

H.Grabner, M.Grabner, H.Bischof, "Real-Time Tracking via On-line Boosting", in *Proc. BMVC*, pp.47-56, 2006.

H.Grabner, C.Leistner, H.Bischof, "Semi-Supervised On-Line Boosting for Robust Tracking", in *Proc. ECCV 2008*, pp.234-247, 2008.

D.Huttenlocher, G.Klanderman, and W.J.Rucklidge, "Comparing Images using the Hausdorff Distance", in *IEEE Trans. on Pattern Analysis and Machine Intelligence*, Vol. 15, No. 9, pp. 850-863, 1993.

Z.Kim, J.Malik, "Fast Vehicle Detection with Probabilistic Feature Grouping and its Application ot Vehicle Tracking", in *Proc. ICCV*, pp.524-531 2003.

D.Koller, J.Weber, J.Malik, "Robust Multiple Car Tracking with Occlusion Reasoning", in *proc. ECCV*, Vol.A, pp.189-196, 1994.

V.Mahadevan, N.Vasconcelos, "Salliency-based Discriminant Tracking", in *Proc.of CVPR 2009*, pp.1007-1013, 2009.

A. Mohan, C. Papageorgiou, and T. Poggio, "Example-based Object Detection in Images by Components", in *IEEE Trans. Pattern Analysis and Machine Learning'*, Vol. 23, No. 4, pp. 349-361, 2001.

K.F. Sim, and K. Sundaraj,. "Human Motion Tracking of Athlete Using Optical Flow & Artificial Markers", in *Proc. ICIAS 2010*, pp. 1-4, 2010.

G.Sundaramoorthi, A.Mennucci, S.Soatto, A.Yezzi, "A New Geometric Metric in the Space of Curves, and Applications to Tracking Deforming Objects by Prediction and Filtering", in *SIAM j. of Imaging Science*, Vol.4, No.1, pp.109-145, 2010.

T.Woodley, B.Stenger, R.Chipolla, "Tracking using Online Feature Selection and a Local Generative Model", in *Proc. BMVC 2007*, 2007.